Materials Physics and Mechanics 38 (2018) 90-110 Received: March 16, 2018

COMPETITION BETWEEN THE VOLUME SOLUTION AND THE SURFACE SEGREGATION OF SOLVED ELEMENTS IN α-Fe

V.P. Filippova[1*], E.N. Blinova[1], A.M. Glezer[1,2], R.V. Sundeev[1,3], A.A. Tomchuk[1,4], L.F. Muradimova[2]

[1]I.P. Bardin Central Research Institute for Ferrous Metallurgy; 23/9-2, Radio str., 105005 Moscow, Russia

[2]National University of Science and Technology "MISiS"; 4, Leninskiy av., 119049 Moscow, Russia

[3]Moscow Technological University "MIREA"; 78, Vernadskogo av., 119454 Moscow, Russia

[4]Bauman Moscow State Technical University; 5-1, 2-nd Baumanskaya str., 105005, Moscow, Russia

*e-mail: varia.filippova@yandex.ru

Abstract. It was experimentally shown, using Auger-spectroscopy method, that there is a certain temperature interval of forming surface segregations of an element (C, N, B, P, Mo, Ti, Al, S, Sn, Cu) solved in α-Fe of low-carbon steels and ferrous-based alloys. Proposed mathematical approach based on traditional relationships of the equilibrium thermodynamics and diffusion kinetics models has determined the temperature scale positions of the intervals of forming segregations of the solved elements in α-Fe.

Keywords: solid solution; surface; segregation; ferrous alloys; kinetics; computer modeling.

1. Introduction

Traditionally, relationships between the values of solved elements concentration in the volume and in the surface (or interface) segregations considered from the equilibrium thermodynamics positions realize the enriched field of an alloy as a separate two-dimensional phase [1], describing the segregation phenomenon as internal adsorption in terms of analogues of gas adsorption on the free surface [2]. From the point of equilibrium thermodynamics, there is no difference between the interface (inter-crystalline or grain boundary) and the surface segregation, because the stimulus of the internal adsorption phenomenon for the both cases is the decrease of the total free energy of the system consisting of the volume plus the surface or the volume plus the interface [1, 2]. Difference between the surface and intercrystalline segregations for solved elements in the same solid solution can be proposed to be of a quantitative kind (in the levels and the rates of achievement of equilibrium concentrations) but not of a qualitative one.

The element concentration as a function of the tempering time after exposing and quenching from higher temperature, $X_b(t)$, is described with the Langmuir curve by analogy with gas adsorption on a free surface, or with the Fowler theory accounting inter-atomic interaction in the segregation field [2, 3, 4]. It looks like a curve with saturation as that one in Fig. 1 (a) presented by M.P. Seah in [4] as the equation (1):

$$\frac{X_b(t)-X_b(0)}{X_b(\infty)-X_b(0)}=1-\exp\left(\frac{FDt}{\beta^2 f^2}\right)\cdot erfc\left(\frac{FDt}{\beta^2 f^2}\right)^{1/2}. \quad (1)$$

The above equation (1) includes the following characteristics: $X_b(t)$ is the segregation level depending on the exposing time (t); $X_b(0)$ is the initial surface concentration equaling to

http://dx.doi.org/10.18720/MPM.3812018_13

the volume one (X_v) of a solved element; $X_b(\infty)$ is the saturation level tied with the limited volume solubility by the value β being the ratio between the volume concentration to the volume solubility; f is the coefficient depending on the difference between the solved and the solute atoms; D is the volume diffusion coefficient, $D = D_0\exp(-Q/RT)$; R is the universal gas constant, R = 8.314 J/(mol.degree); T is the exposing temperature by Kelvin scale; D_0 and Q are the characteristics of the volume diffusivity of a solved element; F=4 for interfaces and F=1 for surfaces [4].

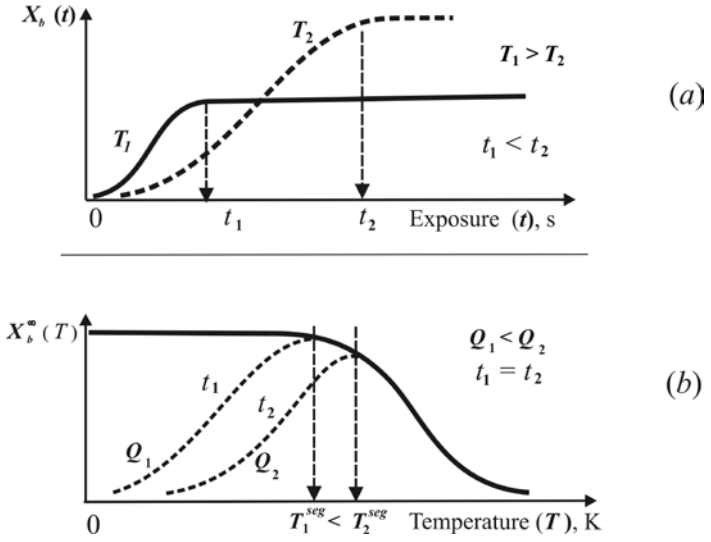

Fig. 1. Relationships of the internal adsorption phenomenon in a solid solution:
a) surface concentration of a solved element ($X_b(t)$) as a function on the tempering time (t);
b) equilibrium surface concentration of a solved element ($X_b^\infty(T)$) as a function on the temperature of isothermal exposing (T).

In general, in spite of some peculiarities of various thermodynamics approaches [1-14], description of the dependence of the equilibrium segregation concentration values, $X_b^\infty(T)$, on those of the volume concentrations (X_v), and the isothermal exposing temperature (T) results in the functions of the following form:

$$\frac{X_b^\infty(T)}{X_v} \sim \frac{X_v}{X_{vo}} \cdot \exp\left(\frac{-\Delta G_{seg}}{RT}\right), \qquad (2)$$

where X_v is the volume concentration and X_{vo} is the limited volume solubility; R is the universal gas constant; ΔG_{seg} is a thermodynamics characteristics of the stimulus of segregations forming. The value ΔG_{seg} further will be named as the "segregation energy" (SE). It should be noted, that segregation of a solved element will take place when SE is positive (ΔG_{seg}>0). It follows from (2) that the level of equilibrium segregation ($X_b^\infty(T)$) is decreasing with the temperature growth. The value of $X_b^\infty(T)$ is directly tied with ΔG_{seg} (according 2). The ratio X_v/X_{vo} in (2) for low soluble impurities, such as S and P in low carbon steels and alloys based on α-Fe, usually being assumed to equal to 1 (one). So, the main factor determining segregations forming to be usually considered is ΔG_{seg}. That one in some works represents the free energy change of the equilibrium segregation forming in the volume-surface (volume-interface) system [5, 6]. Particularly, MacLean evaluated the value ΔG_{seg} in [1] by the elastic energy released at forming the solved atoms segregation. Both surface and interface researching methods are involved for experimental investigation of

segregations [1-15]. Nevertheless, direct experimental measurements of intercrystalline segregations are less available than those ones of free surfaces.

Hondros and Seah [4] proposed a more detailed analogues (3) of the above equation (2) where the limited volume solubility of a low soluble elements in a solid solution to be considered as a function of the temperature $X_{vo}(T)$. So, the relationship (3) including the equilibrium surface concentration (X^{∞}_{b}), the volume concentration (X_v), and the volume solubility (X_{vo}(T)) is the following:

$$\frac{\mathrm{X}_{\mathrm{b}}^{\infty}(T)}{\mathrm{X}_{bo} - \mathrm{X}_{\mathrm{b}}^{\infty}(T)} = \frac{\mathrm{X}_{\mathrm{v}}}{\mathrm{X}_{\mathrm{vo}}(\mathrm{T})} \exp\left[\frac{-\Delta \mathrm{G}_{\mathrm{seg}}}{\mathrm{RT}}\right]. \quad (3)$$

Here, X_{bo} is defined in [4] as the fraction of the enriched surface covered with an atomic layer of a segregating element, that one is a certain reference value (X_{bo} = 2.5÷4.3) characterizing the equilibrium saturated surface thickness having minimum at mono-atomic layer; the values $X^{\infty}_{b}(T)$, X_v , $X_{vo}(T)$ are represented as the molar concentrations). The limited volume solubility is another important characteristics influencing on formation of surface and interface segregations. As it is shown in (2) and (3), the higher is $X_{vo}(T)$ value of a solved element the less is its susceptibility to surface segregation enrichment. And opposite, the less is the limited volume solubility of an element, the higher is its susceptibility to surface enrichment due to internal adsorption. An example of the latter is the brittleness caused by interface segregation of low soluble impurities of P, S, As, etc. in steels [5, 8, 13, 14]. As rule, the limited volume solubility $X_{vo}(T)$ of solved element in α-Fe is increasing with the temperature growth [16, 17], and solving in the volume being the process opposite to segregating in surface or interface [4]. Concluding from the above, the equilibrium segregation value $X^{\infty}_{b}(T)$ as the function on the temperature (2, 3) looks like the monotonic curve (the solid line) represented in Fig.1b, where the value $X^{\infty}_{b}(T)$ is decreasing with the temperature increase.

Summarizing the known kinetics (1) and thermodynamics models (2, 3) of surface (or interface) segregations forming, it is possible to conclude that the higher temperature of isothermal tempering takes place, the smaller value of the saturation level (X^{∞}_{b}) and the lower time of its achievement (*t*) to be observed (Fig.1, a, b). According to the schemes presented in Fig.1 (a, b), the equilibrium segregation level is more rapidly reached under higher exposing temperatures (Fig.1a), but the value of the equilibrium saturation concentration is much less than that could be under lower temperatures (Fig.1b). So, under a limited time of isothermal exposing, one can propose a certain temperature (T_{seg}) of the maximum level of a solved element segregation to exist, as it is shown with dotted curves in Fig.1b. The temperature T_{seg} further being named as “the segregation stability temperature” (SST) is the temperature-scale position of the temperature interval of preferential surface enrichment by the solved element. Certainly, positions of the intervals in the temperature scale for different solved elements can mismatch with each other, depending on relationships between the thermodynamics and kinetics characteristics of the solvent and the solved ones. Again, the process of segregation under real heat treatment conditions in metallurgy involving rather low temperatures and limited time intervals of isothermal expose is controlled by the diffusion rate, then the equilibrium surface concentration values of some solved elements of low diffusion activity to be not reached (dotted curve in Fig.1a). It follows from the latter that surface segregations of more mobile solved elements will form at lower temperatures than those of slower diffusion activity components.

Literature experimental data on temperature intervals of internal adsorption of solved elements in solids are rather poor. Particularly, reversible temper brittleness observed in low- and medium-carbon steels under exposing at (or slow cooling threw) the temperature

750-800 K can be attributed to phosphorous interface segregations forming in α-Fe just in that temperature interval [5-8]. Also, the temperature interval existence for sulfur segregating in the surface of α-Fe near 950 K was experimentally confirmed with Auger-spectroscopy method in work [9].

To study the competition between the elements `solving in the volume and the segregations forming in the surface under isothermal heating and to find the certain temperature intervals of forming the solved elements segregations, the surface of α-Fe alloys under isothermal exposing in vacuum was experimentally investigated in the present work, using Auger-spectroscopy method. For the purpose, there was also used a mathematical analysis of the kinetics and thermodynamics characteristics tied with the obtained time-temperature segregation relationships.

2. Materials and Original Data

For this work realization, there were the original data on thermodynamics and kinetics characteristics influencing volume solubility of impurities and internal surface segregations formation in α-Fe alloys taken from the literature [5, 10-14].

There are the segregation energy values (ΔG_{seg}) of some elements solved in α-Fe presented in Table 1 without differentiation between “internal” and “external” surfaces. The data [5, 10-14] result from either direct measurements of the system energy parameters tied with the equilibrium segregations forming or inverse calculations from relationships similar to (2) using the determined X_b^{∞} / X_v values.

Table 1. Segregation energy values (ΔG_{seg}, kJ/mol) of solved elements in α-Fe based alloys and low-carbon steels, by various scientific References.

[Reference] Solved element	[5]	[11]	[12]	[13]	[14]	[10]
C	92	-	-	88	-	16
P	48	16	83	78	11	25
Mo	0,1	-	0	-	-	5
Cr	0	-	0	-	-	2
Ni	3	-	16	-	3	4
B	-	-	-	-	-	-
S	-	27	-	195	19	38
Sn	-	-	-	-	-	23
Al	-	12	-	-	-	-
Cu	-	-	-	-	-	-
N	-	-	-	112	-	-
Ti	-	-	22	-	-	8

As shown in Table 1, both experimentally determined and simulated ones are just only agree by the order, and thus are only valid for qualitative characterization of the elements segregation possibility. Observed variations of the values of ΔG_{seg} is due to the quantitative evaluations dependence on an accepted physical model and an experimental method of measuring the crystallographic and concentration characteristics of the segregation field (surface or interface). Particularly, the concentration value depends on such segregation characteristics as the inter-crystalline boundary width varying from 1 nm (i.e. about one-two inter-atomic distances measured by transmission electron microscopy method) till 1000 nm (when chemical etching grooves measuring with optical microscopic method takes place).

Again, chemical methods of determination of the average concentrations of the elements in an alloy volume are not able of quantitative characterization of a local segregation composition. From the other side, modern local methods of surface analysis, such as Auger- and X-ray photoelectron spectroscopy, etc. providing registration of elements ratio in a surface layer of several atoms thickness, are not reliable for quantitative estimation of real concentration values but only for qualitative ones [4].

There are the volume solubility of some elements in α-Fe against the temperature, $X_{vo}(T)$, presented in Table 2 from the list square method approximation of the literature data [15, 16]. The high accuracy of the approximation coefficients in Table 2 is due to the computer calculations requirements of attachment of the functions branches. According to the obtained data (Table 2), the volume solubility of the most of the elements solved in α-Fe (S, P, B, Sn, Al, Mo, Cu) is increasing with the temperature growth, being in accordance with the proposition in [4]. Exception of the latter is Mn and Ni, which never were segregating in α-Fe.

Table 2. The limited volume solubility, $X_{vo}(T)$, of some elements in α-Fe as a function on the temperature (T).

Solved Element	The limited volume solubility, $X_{vo}(T)$, 10^{-2} at. %	Temperature interval, T, K
P	$61 \cdot 10^{-5}$ $-0.00232 + T \cdot 10^{-5}$ $0.00015 \cdot \exp(0.00455 \cdot T)$	$T < 293$ $293 \le T \le 773$ $T > 773$
S	$47.943 \cdot \exp(0.001 \cdot T) \cdot 10^{-6}$	$T < 1183$
C	$0.121 \cdot \exp(0.00823 \cdot T) \cdot 10^{-5}$	$T < 1183$
N	$10^{-5} \cdot \exp(0.007 \cdot T)$	$T < 1183$
B	$3.4353 \cdot 10^{-13} \cdot \exp(0.018 \cdot T)$	T <1183
Mo	$0.005 \cdot (1/0.51316 - 0.00028 \cdot T) + (T/(-0.2037 \cdot T + 432.306))$	$T < 1183$
Cr	$0.0019203 \cdot \exp(0.00557 \cdot T)$ $0.01/(0.23766 - 0.00019 \cdot T)$ 1	$T \le 700$ $700 < T \le 1100$ $T > 1100$
Mn	0.035 $0.07365 - 0.00005 \cdot T$ $0.04746 - 0.00002 \cdot T$ $0.1255 - 0.0001 \cdot T$ $0.1935818 - 0.0001636 \cdot T$	$T < 773$ $773 \le T < 873$ $873 \le T < 973$ $973 \le T < 1073$ $1073 \le T < 1183$
Ni	$0.1482935 - 0.0001265 \cdot T$ 0	$T \le 1171.9$ $T > 1171.9$
Sn	$0.0021618 \cdot \exp(0.00317 \cdot T)$	$T < 1183$
Al	$0.086035 \cdot \exp(0.00104 \cdot T)$	$T < 1183$
Cu	$26 \cdot 10^{-8} \cdot \exp(0.008 \cdot T)$ $0.01 \cdot (0.839/\exp(0.044 \cdot T)$	$T \le 1130$ $T > 1130$
Ti	$0.00018 \cdot \exp(0.003 \cdot T)$	$T < 1183$

Table 3. Compositions and parameters of the previous heat treatments (quenching temperature and exposing time) of the investigated alloys based on α-Fe.

Alloy composition (atomic %)	Elements concentration, % (at.)					Quenching temperature (K), Exposing (s)
	P	**S**	**N**	**C**	Other elements, % (at.)	
Fe-0.13P-0.007S-0.025N-0.03C	0.1278	0.007	0.0247	0.0279	0.0579 **Al** 0.0536 **Si**	1153 K, 36000 s
Fe-0.6Al-0.07P-0.005S-0.02N-0.03C	0.0665	0.0052	0.0158	0.0324	0.6185 **Al**	1473 K, 3600 s
Fe-1.2Al-0.05P-0.005S-0.01N-0.04C	0.0501	0.0052	0.0103	0.0369	1.232 **Al**	1473 K, 3600 s
Fe-5.6Al-0.06P-0.007S-0.01N-0.04C	0.0595	0.0068	0.0166	0.0406	5.6228 **Al** 0.01 **Sn**	1473 K, 3600 s
Fe-0.03S-0.14P-0.06N-0.02C-0.005Ti-0.006Cu	0.1441	0.0348	0.0581	0.0186	0.0352 **Ni** 0.0116 **Mo** 0.0047 **Ti** 0.0061**Cu**	1373 K, 600 s
Fe-0.02S-0.14P-0.3N-0.04C	0.1441	0.0209	0.0251	0.0372	0.0494 **Ni** 0.064 **Mo**	1373 K, 600 s
Fe-0.1Sn-0.1P-0.004S-0.006N-0.1C	0.092	0.0044	0.006	0.014	0.0054 **Cr** 0.0619 **Ni** 0.1083 **Sn**	1153 K, 36000 s
Fe-0.6Cr-0.13P-0.004S-0.001N-0.01C	0.1297	0.0035	0.0011	0.0093	0.5901 **Cr**	1139 K, 600 s
Fe-1Cr-0.13P-0.004S-0.002N-0.01C	0.1314	0.0035	0.0032	0.0093	1.3725 **Cr**	1139 K, 600 s
Fe-1Mo-0.16P-0.004S-0.014N-0.02C	0.1596	0.0035	0.014	0.0234	0.9954 **Mo** 0.05 **Si**	1139 K, 600 s
Fe-3Mo-0.26P-0.004S-0.06N-0.03C	0.2648	0.0036	0.0626	0.0285	3.1172 **Mo** 0.0974 **Si**	1139 K, 600 s
Fe-3Mo-0.15P-0.004S-0.1N-0.01C	0.1545	0.0044	0.1053	0.0142	3.0816 **Mo** 0.1014 **Si**	1139 K, 600 s
Fe-0.02B-0.07P-0.005S-0.03N-0.02C	0,072	0.0052	0.0263	0.0186	0.19 **Ni** 0.0155 **B** 0.133 **Si**	923 K, 5400 s
Fe-0.03B-0.02P-0.007S-0.04N-0.02C-2.7Ni	0.0197	0.0069	0.0369	0.0231	2.7458 **Ni** 0.0257 **B** 1.049 **Si**	923 K, 5400 s
Fe-0.002B-0.13P-0.005S-0.003N-0.03C	0.1259	0.0052	0.0032	0.278	0.1234 **Ni** 0.0021 **B** 0.0456 **Si**	923 K, 5400 s
Fe-1Ni-0.14P-0.005S-0.06N-0.01C	0.1405	0.0052	0.0562	0.0093	0.9126 **Ni**	1153 K, 36000 s
Fe-3Ni-0.03P-0.005S-0.003N-0.014C	0.0343	0.0052	0.0028	0.014	3.0955 **Ni**	1153 K, 36000 s
Fe-3Ni-0.17P-0.007S-0.05N-0.014C	0.1731	0.007	0.0514	0.014	2.9495 **Ni**	1153 K, 36000 s

In the present work, the investigated alloys compositions and the previous heat treatment conditions were resulted from analysis of the above data presented in Tables 2. The binary and ternary Fe-based alloys involving P and S (as main impurities inducing brittleness of steels) and one of the alloying element (Mo, Cr, Ni, B, or Al) considered as a potential tool of neutralization of P and S segregations were prepared for the investigation. The original specimens were thin square (10x10 mm) plates of 0.5 mm thickness previously quenched in

water. There were quenching temperatures chosen to provide maximal solution of the involved components in α-Fe. There are the compositions of the investigated alloys, the exposing duration and the temperatures of previous quenching presented in Table 3.

The volume diffusivity characteristics (D_0, Q) of some elements solved in α-Fe there are presented in Table 4 involving the data from [17-27]. As shown in Table 4, the diffusion activation energy values (Q) of C, N, and B solved in α-Fe are approximately by 3-4 times lower than of P, Mo, Ti, Al, S, Sn, and Cu. According to (1), Fig.1b, we can propose a high segregation level of C, N, and B to develop at lower temperatures than of P, Mo, Ti, Al, S, Sn, Cu.

Table 4. Parameters of the volume diffusion coefficient, D, for solved elements in α–Fe based alloys and low-carbon steels: $D = D_0\exp(-Q/RT)$.

Solved Element	D_o, 10^{-4} m^2/s	Q,		Ref.
		kcal/mol	**kJ/mol (*)**	
C	0.0251 ± 0.01	18.3 ± 0.8	76.7 ± 3.4	[17]
N	0.00144	17.7± 0.1	74.3 ± 0.4	[18]
B	0.0023	19 ± 2	79.6 ± 8.4	[19]
P	376	65.6 ± 0.5	275.0 ± 2.1	[20]
Mo	0.44	57.0 ± 0.5	238.8 ± 2.1	[21]
Cr	2.53	57.5 ± 0.5	240.9 ± 2.1	[22]
Ni	0.6	62.6 ± 0.6	262.3 ± 2.5	[21, 23]
S	1700	61.2 ± 0.5	256.4 ± 2.1	[24]
Sn	8	61.2 ± 0.5	256.3 ± 2.1	[25]
Al	5.9	57.7 ± 1.0	241.8 ± 4.2	[23]
Cu	6	59 ± 1	247.2 ± 4.2	[26]
Ti	20	58 ± 1	243.0 ± 4.2	[27]

* The literature data related to common conditions (1 kJ/mol = 4.19 kcal/mol).

3. Experimental methods

To study kinetics of internal adsorption of solved elements in α-Fe under isothermal exposing, there was using the Auger-spectroscopy method of surface concentration determination with a combine-spectrometer ESCALAB MK-2 of VG firm (UK). Every investigated specimen was previously cleaned by scraping inside the spectrometer preparation chamber, providing vacuum about 10^{-8} Pa, and then situated in the working chamber, where was heated from the room temperature and exposed at a certain constant temperature (from 300 K to 950K) during several hours (1, 2 or 3 h), vacuum being not worse than 10^{-7} Pa.

The Auger spectra were recorded in the time intervals with duration from 10 minutes to 2 hours, depending on exposing temperature influencing the segregating rate. The recording regimes were chosen from the principles described in [4] to provide high expressivity combined with a satisfactory resolution for analysis of thin electron spectrum structure at the required conditions of the heat treatment in vacuum. So, the recording mode was CRR = 4 with rate of 0.2 eV·s^{-1} order; primary electron energy E = 3000 eV; $\Delta E/E = const$; the baseband voltage being of 5.0 V. Thickness of the analyzed layer under considered conditions is about 5 atomic sizes, that is comparable with the escape depth of ferrous atoms Auger-electrons having binding energy of 703 eV. For quantitative analysis of elements concentrations in segregation (X^i_b) we used the computational procedure developed in [6]. Here, surface-volume ratio of atomic concentrations (X^i_b/X^i_v) of an element i was equated with the ratio of the intensities of relevant Auger-peaks of the element before and after isothermal exposing, considering that as the ratio of the volume and the surface concentrations. The

volume concentrations values (X^i_v) determined previously by the standard chemical analysis (Table 4) of the alloys under investigation were considered as the etalons for computing the surface compositions from Auger-spectroscopy data. The details of the Auger spectroscopy investigation were the same as those published in [28].

4. Experimental Results

The isotherms of nitrogen, carbon, sulfur, and phosphorus adsorbing on the surface of one of the investigated alloys (Fe-0.13P-0.007S-0.025N-0.03C) under isothermal exposing in vacuum of the Auger-spectrometer working chamber are presented (atomic %) in Fig. 2. The following peculiarities of the elements surface segregation under isothermal exposing of the considered alloy in vacuum can be observed: surface enrichment by carbon runs at relatively low temperatures (till 600 K); nitrogen segregation develops in the temperature interval 500-600 K; phosphorus appreciably enriches the surface at temperatures 550-650 K; sulfur begins creating segregations from 600 K and upper.

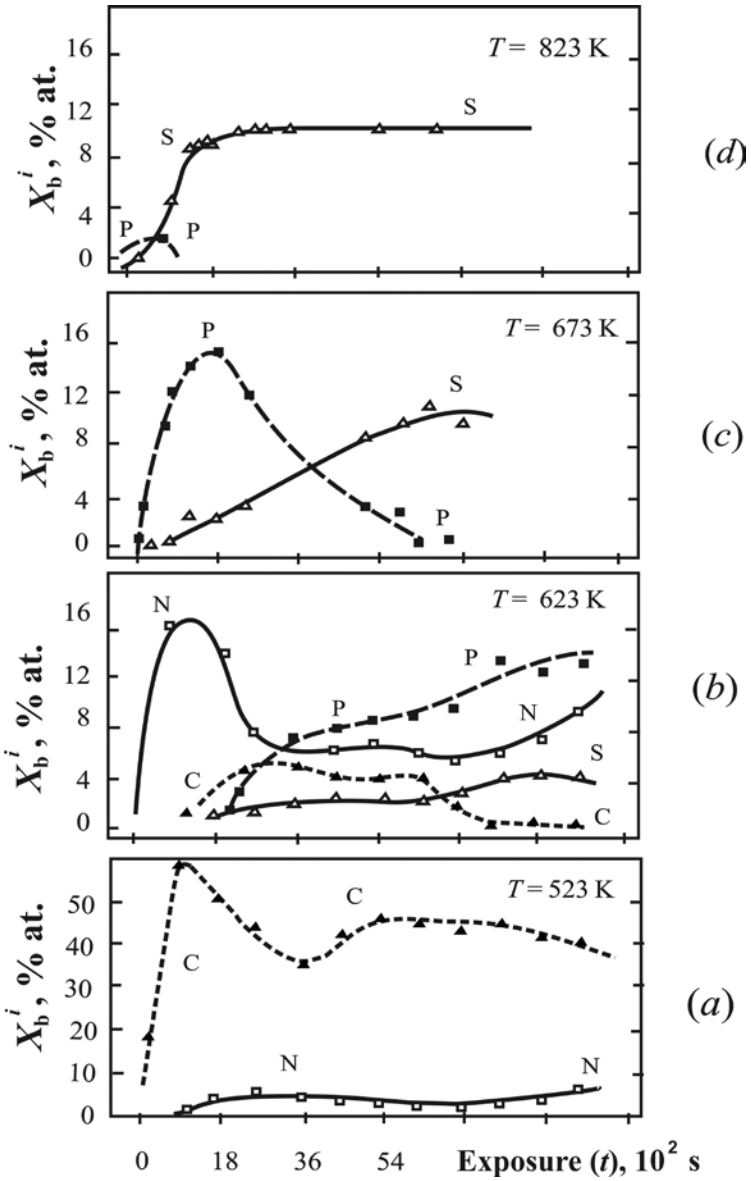

Fig. 2. Isotherms of forming surface segregations of nitrogen (N), carbon (C), sulfur (S), and phosphorus (P) in alloy Fe-0.13P-0.007S-0.025N-0.03C (%, at.) under isothermal exposing in vacuum at various temperatures: a) 523 K; b) 623 K; c) 673 K; d) 873 K.

The experimental results on internal adsorption of N, C, S, and P in the surface of Fe-0.13P-0.007S-0.025N-0.03C (%, at.) alloy described above (Fig. 2) are also shown in Fig. 3 as the time-temperature concentration diagrams (TTC-diagrams), where C-curves represent the time of about 50%-75% level of equilibrium segregation attainment. Analogous diagrams for the solved elements forming segregations in Fe-based alloys are shown in Figs. 4-10. The lower branches of the C-curves represent reduction of the time of segregation forming against the exposition temperature growth, the relationship observed being tied with atomic diffusivity increasing. After the exposing temperature has grown till some value, the equilibrium level of segregation goes down (Fig. 1 a), and the time of forming segregation of a considered enrichment level extremely increases (the upper brunches of the C-curves in Figs. 3-10).

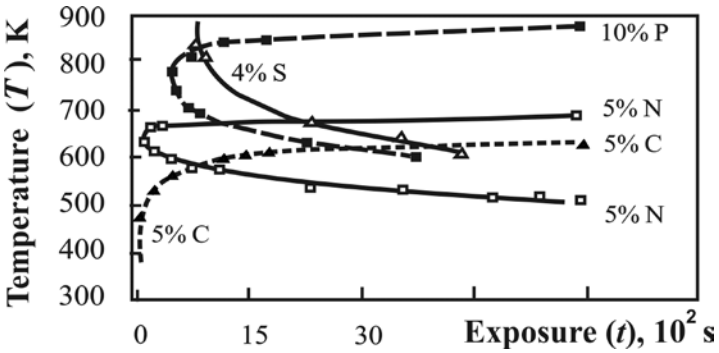

Fig. 3. Time-temperature concentration diagrams of forming 50% level of equilibrium segregations of P, S, N, and C in the free surface under isothermal exposing in vacuum of the alloy: Fe-0.13P-0.007S-0.025N-0.03C (%, at.).

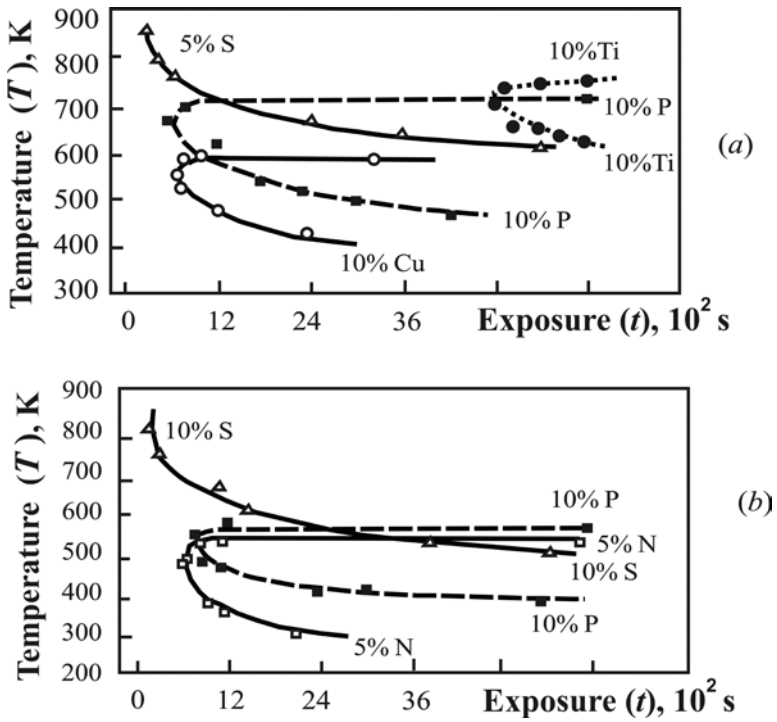

Fig. 4. Time-temperature concentration diagrams of forming 50% level of equilibrium segregations of P, S, N, C, Ti and Cu in the free surface under isothermal exposing in vacuum of the Fe-S-P alloys: a) Fe-0.03S-0.14P-0.06N-0.02C-0.005Ti-0.006Cu;
b) Fe-0.02S-0.14P-0.3N-0.04C (%, at.).

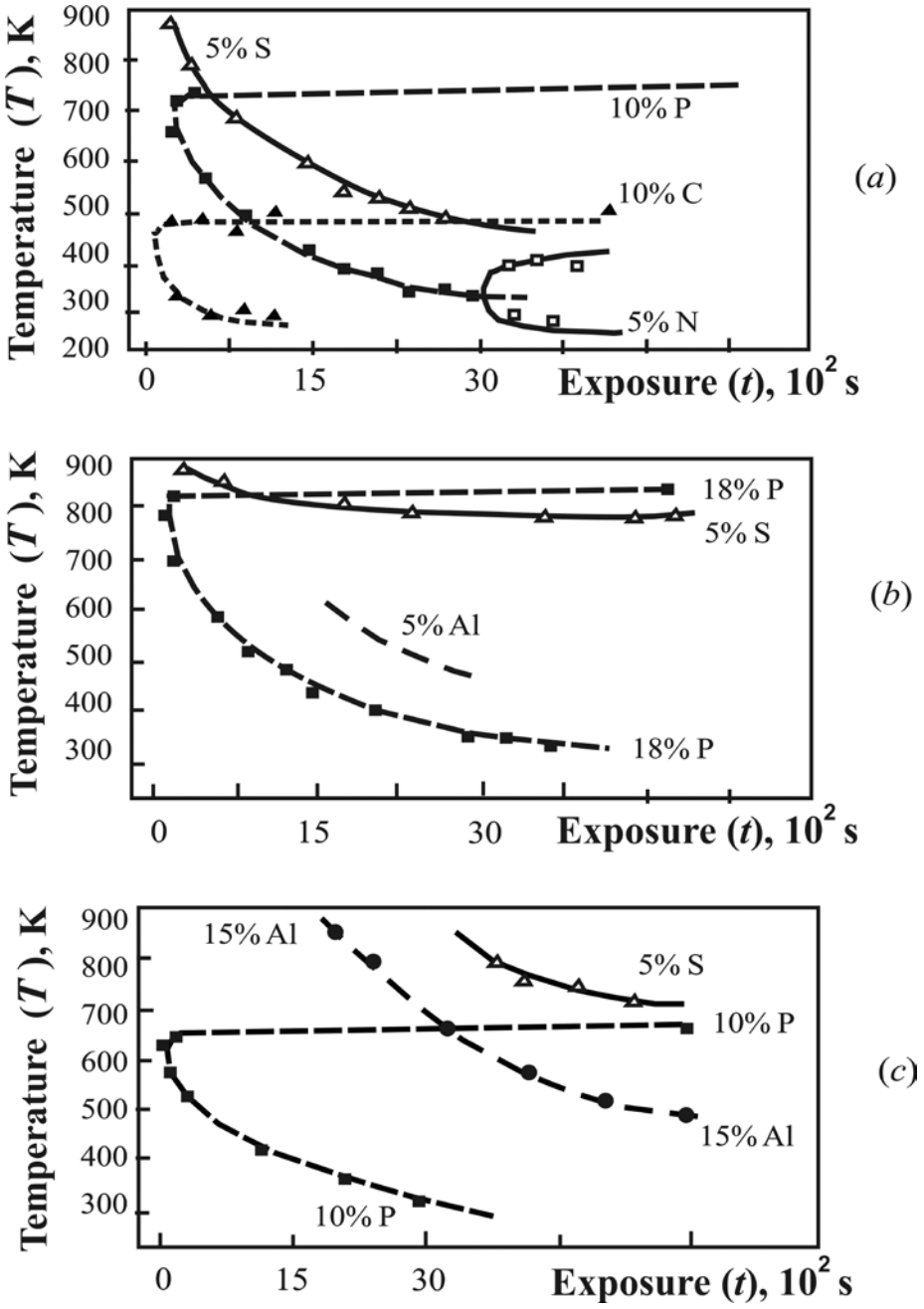

Fig. 5. Time-temperature concentration diagrams of forming 50% level of equilibrium segregations of P, S, N, C, and Al in the free surface under isothermal exposing in vacuum of the Fe-Al-P alloys: a) Fe-0.Al-0.07P-0.005S-0.02N-0.03C;
b) Fe-1.2Al-0.05P-0.005S-0.01N-0.04C; c) Fe-5.6Al-0.06P-0.007S-0.01N-0.04C (%, at.).

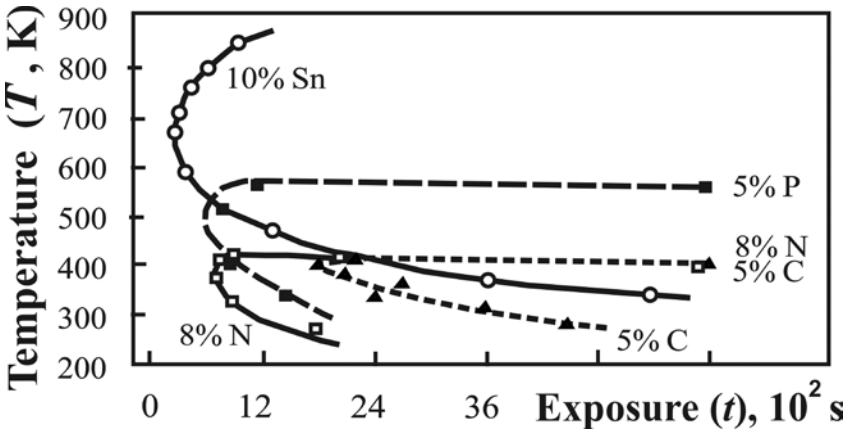

Fig. 6. Time-temperature concentration diagrams of forming 50% level of equilibrium segregations of P, N, C, and Sn in the free surface under isothermal exposing in vacuum of the Fe-Sn-P alloy: Fe-0.1Sn-0.1P-0.004S-0.006N-0.1C (%, at.).

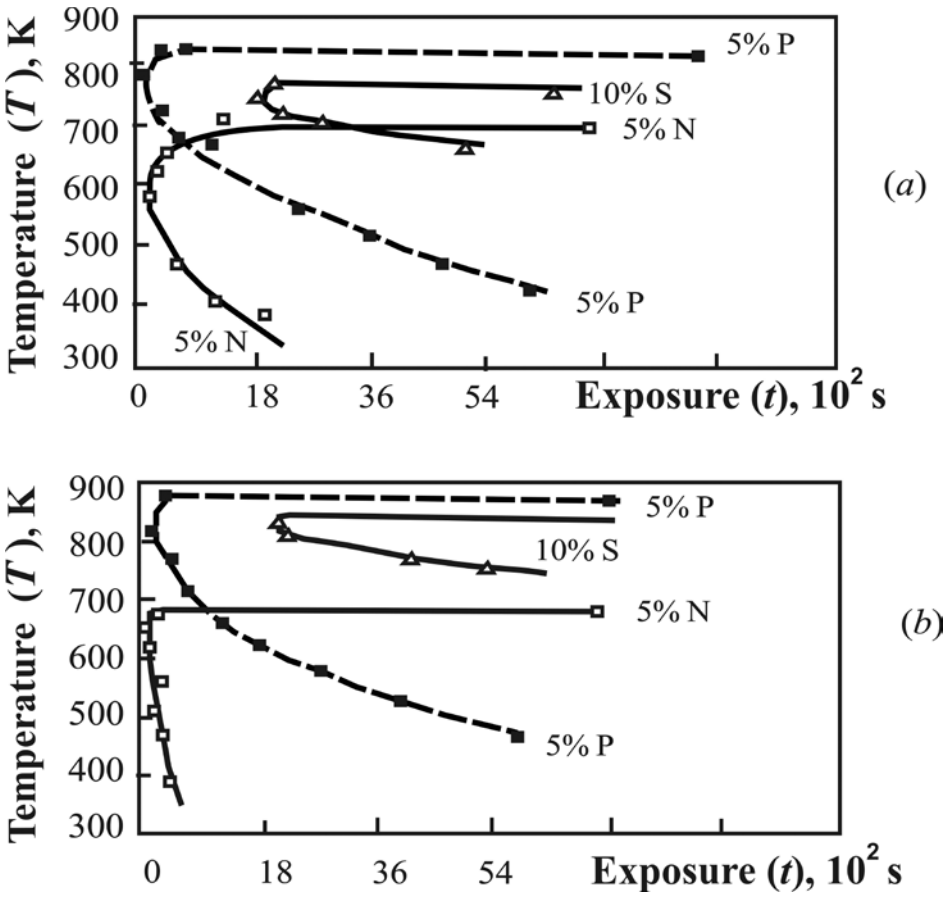

Fig. 7. Time-temperature concentration diagrams of forming 50% level of equilibrium segregations of P, S, and N in the free surface of the Fe-Cr-P alloys under isothermal exposing in vacuum:
a) Fe-0.6Cr-0.13P-0.004S-0.001N-0.01C; b) Fe-1Cr-0.13P-0.004S-0.002N-0.01C (%, at.).

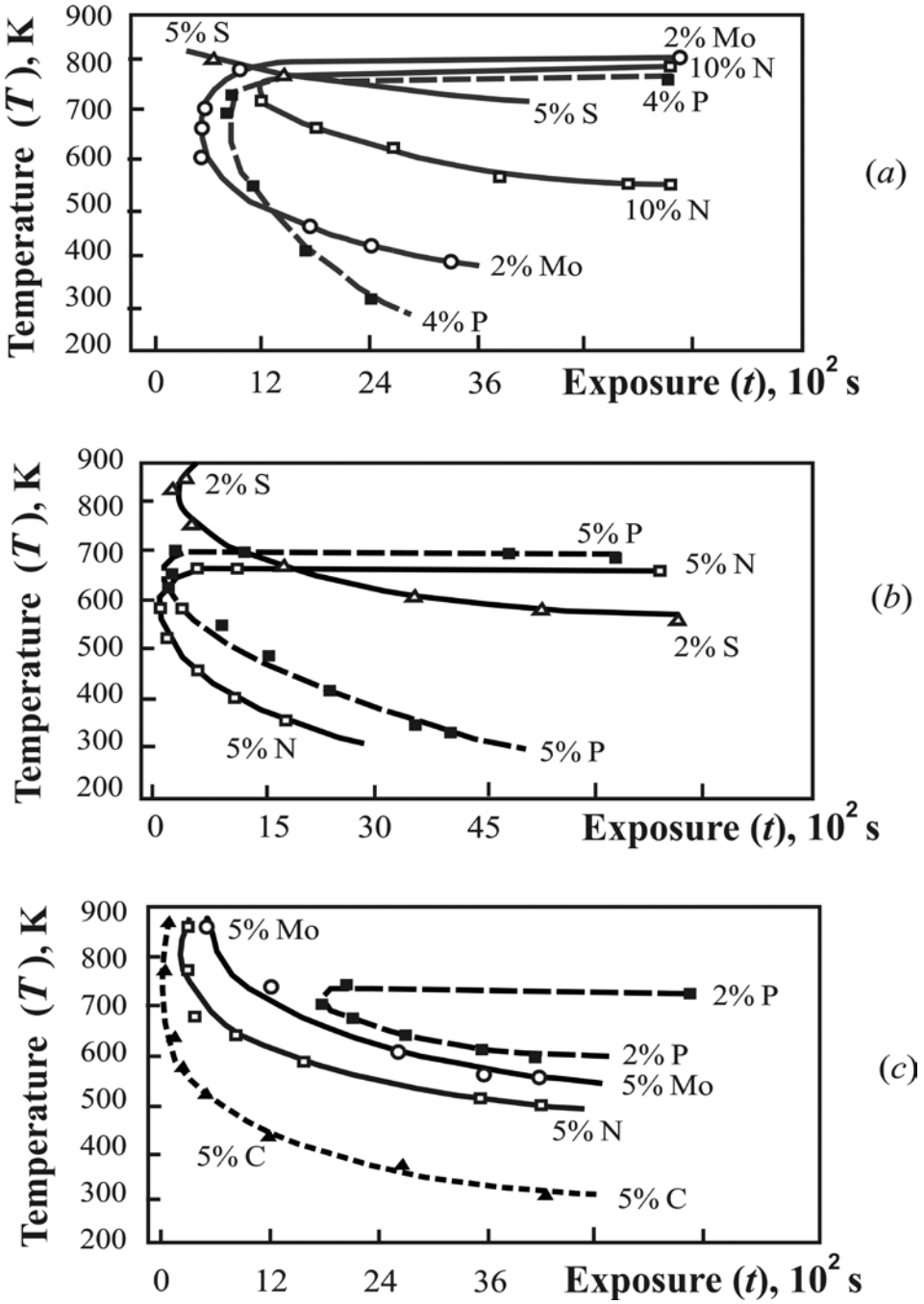

Fig. 8. Time-temperature concentration diagrams of forming 50% level of equilibrium segregations of P, S, N, C, and Mo in the free surface under isothermal exposing in vacuum of the Fe-Mo-P alloys:
a) Fe-1Mo-0.16P-0.004S-0.014N-0.02C; b) Fe-3Mo-0.26P-0.004S-0.06N-0.03C;
c) Fe-3Mo-0.15P-0.004S-0.1N-0.01C (%, at.).

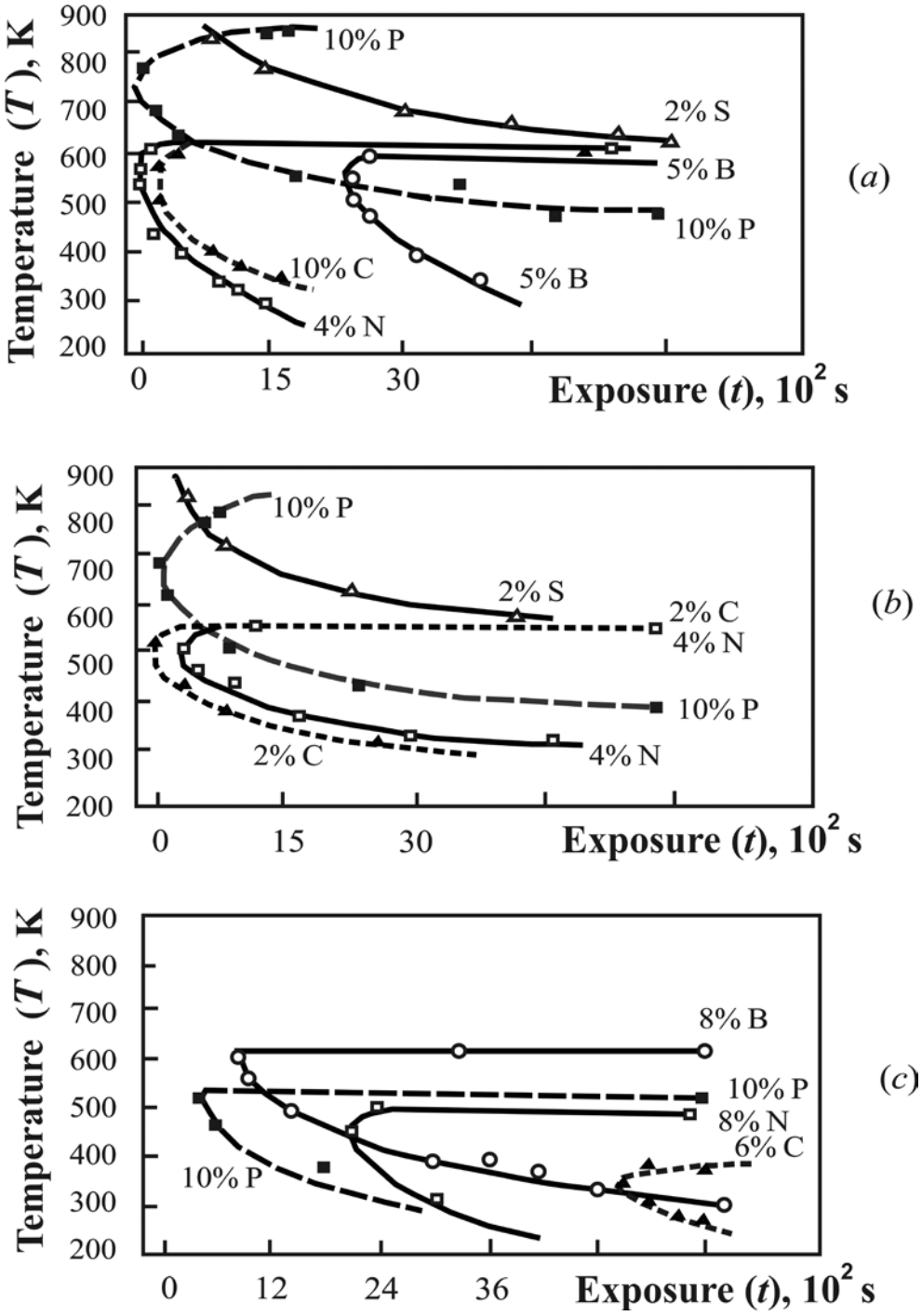

Fig. 9. Time-temperature concentration diagrams of forming 50% level of equilibrium segregations of P, S, N, C, and B in the free surface under isothermal exposing in vacuum of the Fe-B-P alloys:
a) Fe-0.02B-0.07P-0.005S-0.03N-0.02C; b) Fe-0.03B-0.02P-0.007S-0.04N-0.02C-2.7Ni;
c) Fe-0.002B-0.13P-0.005S-0.003N-0.03C (%, at.)

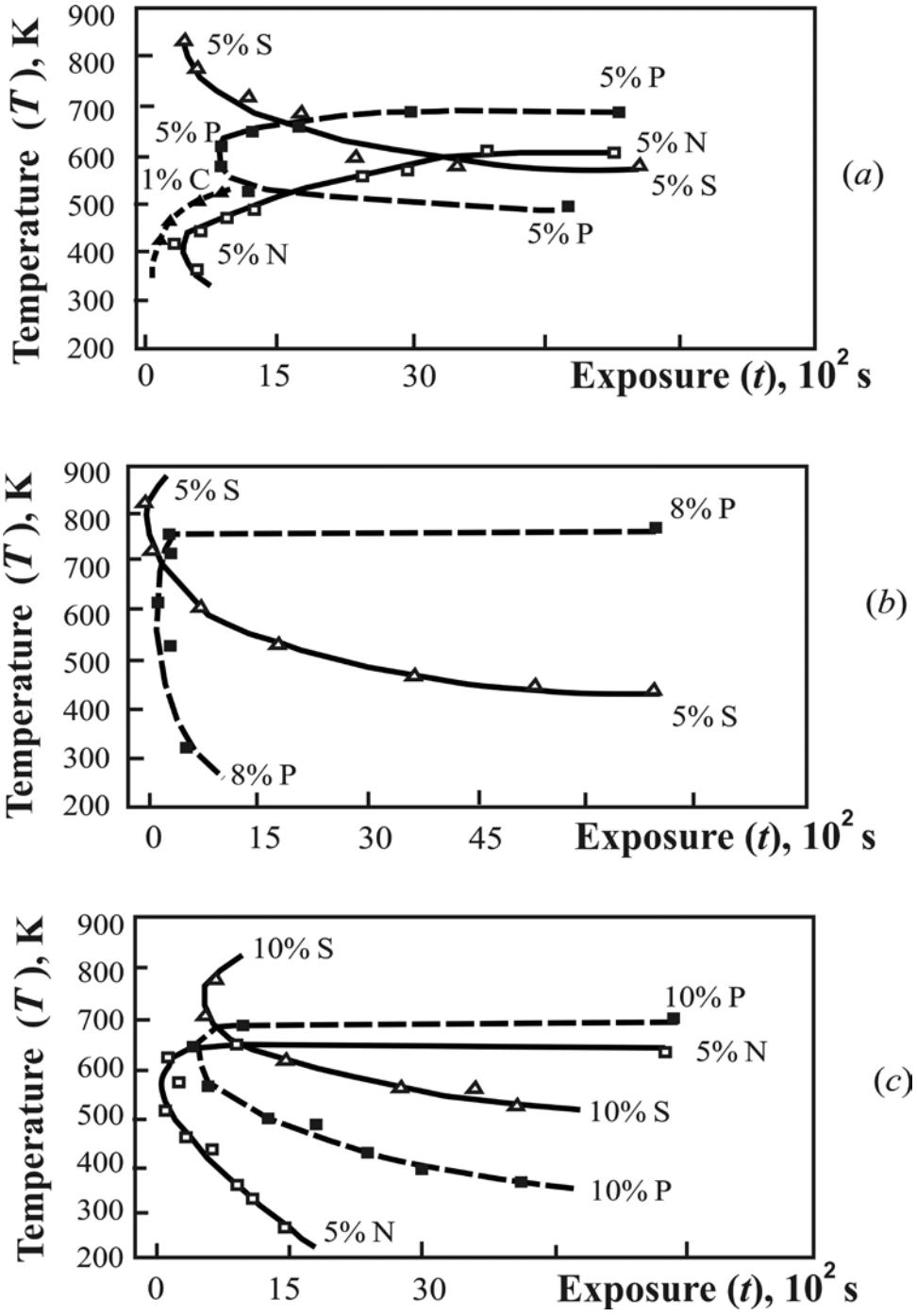

Fig. 10. Time-temperature concentration diagrams of forming 50% level of equilibrium segregations of P, S, N, and C in the free surface under isothermal exposing in vacuum of the Fe-Ni-P alloys:
a) Fe-1Ni-0,14P-0,005S-0,06N-0,01C; b) Fe-3Ni-0.03P-0.005S-0.003N-0.014C;
c) Fe-3Ni-0.17P-0.007S-0.05N-0.014C (%, at.).

From the experimental data presented in Fig.3-10, one can observe the following temperature peculiarities of soled elements segregations forming in the surface of α-Fe alloys under isothermal exposing in vacuum.

- Surface enrichment with carbon (C) presents in investigated alloys at low temperatures (lower than 600 K).

- Nitrogen (N) segregates in the temperature intervals close to 500 K -650 K.
- Segregations of a maximal concentration of P are observed near one the same temperature (closed to 800 K) coinciding with that of the known reversible temper brittleness interval of low-carbon steels (770-830 K), that was discussed in [7, 8].
- Segregations of S, Al, and Sn develop in the same temperature interval (800-950 K) having position upper than that of P (Fig. 4, 5, 6). Again, Al is segregating together with S (Fig. 5 c); while Sn displacing S, and surface segregation of the latter not forming in spite of that one presenting in the alloy volume (Fig. 6).
- With increase of the volume concentration of Cr, the temperature of P segregation formation grows (Fig. 7), while Al reducing the latter (Fig. 5).
- Influence of Al on segregation development in α-Fe based solid solutions has a complicated mechanism: low concentrations of Al sharply eliminate surface segregations of N and C (Fig. 5 a, b), the latter promoting surface activation of P by that way; with Al volume concentration increasing, the formation temperature and maximum concentration of P segregation are decreasing (Fig. 5 c).
- Segregations of Mo, Ti, and P are forming approximately in the same temperature interval (Figs. 4, 8). But, with increasing the volume concentrations of N and Mo, the temperatures of forming N, C, and Mo segregations grow up to 900K (Fig. 8 c).
- Segregations of B and Cu arise at the same temperature interval as N and C (Fig. 4 a , and Fig. 9 a, b, c)
- Nickel (Ni) eliminates segregation of boron (B) (Fig. 9 b).
- Segregations of Ni in the α-Fe alloys are absent (Figs. 3-10 a, b, c).

There are the segregation forming temperatures (SFT) from the “nose” positions of the equal-concentration curves (Figs. 3-10) for the elements solved in the investigated α-Fe alloys presented in Fig. 11 as gray rectangles having the length corresponding to the results scattering. The segregating elements are disposed along horizontal direction in the order of increase of the arithmetical average means of T_{seg} values (black points). The length of the gray rectangles for Cu, Ti, and Sn corresponds to the experimental accuracy of the Auger-spectroscopy method used: $\Delta T_{seg} = \pm 25$K.

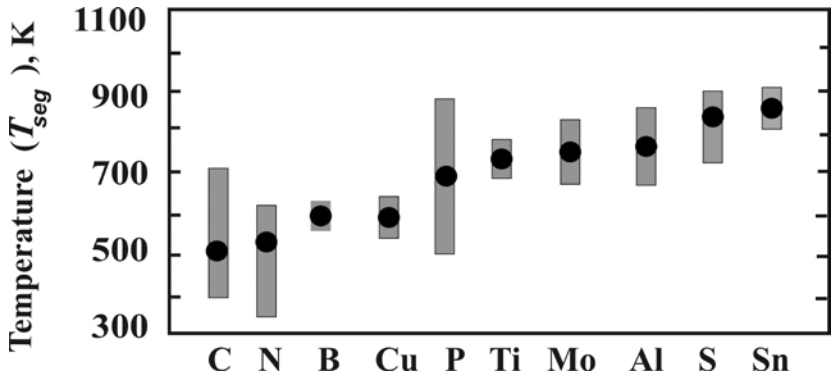

Fig. 11. The segregation forming temperatures (T_{seg}) of the elements solved in the investigated α-Fe alloys, from Auger-spectroscopy data: the gray rectangles have got the length corresponding to the results scattering; the black points are the arithmetical average means of the experimental T_{seg} values.

One can observe a certain relationship between experimental values of T_{seg} (Fig. 11) and the diffusion activation energy of the solved elements in α-Fe (Table 4): C, N, and B, having lower volume diffusion activation energies (Q), form interface segregations at lower

temperatures T_{seg} than those having Q values approximately 3-4 times higher (P, Mo, Ti, Al, S, Sn). The only exclusion is Cu.

5. Discursion of the results and the simulation model

Table 5. The values of the surface segregation temperature corresponding to C-curves "nose" positions (T_{seg}, K) with the accuracy of ±25K in the time-temperature concentration diagrams (Fig.3-10) for the investigated α-Fe based alloys during isothermal exposing in vacuum (bold type, an upper line); the values of $-\Delta G_{seg}$ (kJ/mol) computed from the Auger-spectroscopy data (a lower line).

Fig	Alloy volume composition (at.%)	**C**	**N**	**B**	**P**	**S**	**Mo**	**Al**	**Ti**	**Cu**	**Sn**
2, 3	Fe-0.13P-0.007S-0.025N-0.03C	**470** 16	**630** 25	X	**750** 22	**800** 5	X	X	X	X	X
4 (a)	Fe-0.03S-0.14P-0.06N-0.02C-0.005Ti-0.006Cu	-	-	X	**680** 19	**900** 7.5	X	X	**710** 13	**590** 24	X
4 (b)	Fe-0.02S-0.14P-0.3N-0.04C	-	**500** 15	X	**550** 7	**820** 5.8	X	X	X	X	X
5 (a)	Fe-0.6Al-0.07P-0.005S-0.02N-0.03C	**420** 14	**350** 7	X	**700** 20	**900** 7.5	X	-	X	X	X
5 (b)	Fe-1.2Al-0.05P-0.005S-0.01N-0.04C	-	-	X	**820** 27	**900** 7.5	X	**650** 3	X	X	X
5 (c)	Fe-5.6Al-0.06P-0.007S-0.01N-0.04C	-	-	X	**620** 16	**800** 5.5	X	**850** 6	X	X	X
6	Fe-0.1Sn-0.1P-0.004S-0.006N-0.1C	**400** 11	**400** 10	X	**550** 7	-	X	X	X	X	**850** 20
7 (a)	Fe-0.6Cr-0.13P-0.004S-0.001N-0.01C	-	**600** 22	X	**780** 24	**750** 4.5	X	X	X	X	X
7 (b)	Fe-1Cr-0,13P-0,004S-0,002N-0,01C	-	**610** 23	X	**870** 30	**840** 6	X	X	X	X	X
8 (a)	Fe-1Mo-0.16P-0.004S-0.014N-0.02C	-	**710** 30	X	**700** 22	**850** 6	**650** 8	X	X	X	X
8 (b)	Fe-3Mo-0.26P-0.004S-0.06N-0.03C	-	**600** 22	X	**650** 17	**800** 5.5	-	X	X	X	X
8 (c)	Fe-3Mo-0.15P-0.004S-0.1N-0.01C	**690** 26	**750** 35	X	**700** 20	-	**800** 10	X	X	X	X
9 (a)	Fe-0.02B-0.07P-0.005S-0.03N-0.02C	**590** 25	**590** 21	**550** 50	**750** 22	**820** 5.8	X	X	X	X	X
9 (b)	Fe-0.03B-0.02P-0.007S-0.04N-0.02C-2.7Ni	**520** 20	**520** 15	-	**750** 22	-	X	X	X	X	X

9 (c)	Fe-0.002B-0.13P-0.005S-0.003N-0.03C	**380** 10	**480** 14	**610** 60	**510** 6	-	X	X	X	X	X
10 (a)	Fe-1Ni-0.14P-0.005S-0.06N-0.01C	**460** 15	**460** 15	X	**600** 10	**850** 6	X	X	X	X	X
10 (b)	Fe-3Ni-0.03P-0.005S-0.003N-0.014C	-	-	X	**750** 22	**900** 7.5	X	X	X	X	X
10 (c)	Fe-3Ni-0.17P-0.007S-0.05N-0.014C	-	**590** 21	X	**650** 17	**780** 5	X	X	X	X	X

(X) – the element is absent in the alloy volume composition;
(-) – segregation of the element was not observed in the considered temperature interval: 300 ÷1000K.

From the Hondros and Seah equation (3), using the additive approach proposed by Guttmann for multi-component systems [12], we can represent the equilibrium concentration of the *i*-th component as the temperature function, $X^{\infty}{}_b{}^i(T)$:

$$\frac{X_b^{\infty i}(T)}{X_{bo} - \sum_{i=1}^{N} X_b^{\infty i}(T)} = \frac{X_v^i}{X_{vo}^i(T)} \exp\left[\frac{-\Delta G^i{}_{\text{seg}}}{RT}\right]. \quad (4)$$

From the latter, we can appreciate the segregation energy values (ΔG^i_{seg}) for the solved components of the investigated alloys from the experimental data of this work (Figs. 3-10). To find the ΔG^i_{seg} value for every *i*-the element of a multi-component alloy in the present work, the concentration observed at maximal expositions (about 7200 s) with the constant temperature $T=T^i_{seg}$ (Figs. 3-10) being considered as the saturated level ($X^{\infty}{}_b{}^i(T)$) localized in the layer of two-atomic thickness (X_{bo}= 2). The limiting volume solubility values (X^i_{vo}) were the temperature functions presented in Table 2. There are the resultant values of ΔG^i_{seg} and T_{seg} from Auger-spectroscopy presented in the above Table 5. For the latter, one can observe an order-of-magnitude agreement of the obtained ΔG^i_{seg} values with the literature data in Table 1 both for surface and interface segregations.

Considering SFT (Table 5) as analogous of SST (Fig. 1b), the value T_{seg} can be mathematically determined from the maximum condition of the concentration-temperature function described with the equation (3) accounting temperature dependence of the volume solubility, as shown further.

As known, the maximum (extreme) condition of a function is equality to null of its derivative. The latter for relationship (4) looks as the following:

$\partial X^{\infty}{}_b{}^i(T)/\partial T = 0.$ (5)

Obviously, the precise solution of equation (5) for the function $X_b^{\infty}(T)$ in form of (3) does not exist, because the latter is a monotonic one similar to the solid line shown in Fig. 1, b. However, it is possible to find an approximate solution of (5) for the latter if consider conditions of the concentration $X_b{}^i(T)$ being close to saturation (at rather low temperatures and enough long time period of the isothermal exposing). Thus, we believe the following to be true:

$X^i{}_b(T) \cong X^{\infty}{}_b{}^i(T) = const$ and $\partial X^i{}_b(T)/\partial T \cong 0$.

The segregation concentration ($X^{\infty}{}_b{}^i(T)$) and the limiting volume solubility ($X_{vo}{}^i(T)$) are functions on the temperature. Another parameters in (4) are assumed to be independent on the

temperature: the number of segregating components of the solid solution (N); the structure and the total number of the atomic places in the segregation ($X_{bo} = const$); the thermodynamics stimulus for segregating ($\Delta G^{i}_{seg}/R = const$); volume concentrations of the components ($X_v^{\,i} = const$). Also, from the relationship ($\sum_{i=1}^{N} X_b^{\infty i}(T) = 1$) proposed above in (4), it follows that: $X_{bo} - \sum_{i=1}^{N} X_b^{\infty i}(T) = const.$

Differentiating the left and the right part of the equation (4) with respect to the temperature T on the above assumptions and condition (5), we receive the following equation (6) to find $T = T^{i}_{seg}$:

$$\frac{\partial X_b^{\infty i}(T)}{\partial T} = \left(X_{bo} - \sum_{i=1}^{N} X_b^{\infty i}(T) \right) \cdot X_v^{\,i} \cdot \frac{\partial}{\partial T} \left(\frac{1}{X^{i}_{vo}(T)} \exp\left(\frac{-\Delta G^{i}_{seg}}{RT} \right) \right) = 0 . \tag{6}$$

Obviously, the equation (6) will have solutions only under condition of equality to zero of the third multiplier being the derivative of a composite function; using transformation rules of the latter, we obtain the following (7):

$$-\frac{1}{(X^{i}_{vo}(T))^2} \cdot \frac{\partial X^{i}_{vo}(T)}{\partial T} \cdot \left(\exp\left(\frac{-\Delta G^{i}_{seg}}{RT} \right) \right) + \frac{1}{X^{i}_{vo}(T)} \cdot \left(\exp\left(\frac{-\Delta G^{i}_{seg}}{RT} \right) \right) \cdot \left(\frac{\Delta G^{i}_{seg}}{RT^2} \right) = 0 . \tag{7}$$

Accounting that $\frac{1}{X^{i}_{vo}(T)} \cdot \left(\exp\left(\frac{-\Delta G^{i}_{seg}}{RT} \right) \right) \neq 0$, we transform (7) to the following shape (index i further will be omitted):

$$-\frac{1}{X_{vo}} \frac{\partial X_{vo}(T)}{\partial T} + \frac{\Delta G_{seg}}{RT^2} = 0 . \tag{8}$$

The equation for estimation of SST ($T=T_{seg}$) results from (8) as (9):

$$T_{seg}^{\,2} = \frac{\Delta \mathrm{G}_{\mathrm{seg}}}{\mathrm{R}} \left[\mathrm{X}_{\mathrm{vo}}(T) \Big/ \left(\frac{\partial \mathrm{X}_{\mathrm{vo}}(T)}{\partial T} \right) \right] . \tag{9}$$

Analysis of the equation (9) for the possibility of existing of its solution for T results in the following conclusions. Firstly, solution of (9) for $\mathrm{T}=T_{seg}$ being positive by physical interpretation, as the absolute temperature ($T_{seg}>0$), can exist only if the two conditions simultaneously hold: 1) $\Delta G_{seg}>0$, that is thermodynamics condition of the element equilibrium segregation forming; 2) the volume solubility of the element is increasing with the temperature, that is $\partial X_{vo}(T)/\partial T>0$. The latter condition, according to the literature data (Table 2), is valid for the most of elements solved in α-Fe (S, P, B, Sn, Al, Mo, Cu) but Mn and Ni. The volume solubility of the last ones decreases with the temperature growth. In that case, obviously, equation (9) does not have solutions in the field of $T_{seg} > 0$. Secondly, it follows from (9) that SST ($T=T_{seg}$) grows when the value of ΔG_{seg} increases. The latter circumstance can be weighty for development of heat treatment conditions preventing harmful impurities segregation in low-carbon steels and Fe-based alloys, proposing that external and internal surfaces to be identical in case of the internal adsorption phenomenon under consideration. Thirdly, absolute accuracy of the volume solubility temperature data ($X_{vo}(T)$) presented by the list square method approximation in Table 3 [15, 16] is not of so great importance for the fulfilled simulations, as the term inside the square brackets of (9) is nothing less than the relative change of the volume solubility $X_{vo}(T)$ in respect of the temperature.

Solution of the equation (9) for T_{seg} can be found by the step-by-step approaching method. For this, (9) transforms into (10) by the following manner:

$$(T_{seg})_{j+1} = \sqrt{\frac{\Delta G_{seg} X_{vo}(T_j)}{R} \Big/ \frac{X_{vo}(T_j + \Delta T) - X_{vo}(T_j)}{\Delta T}}, \; j = 1, 2, 3, 4, \qquad 10)$$

The calculations realized in this work have shown that the equation (10) has a satisfactory convergence for α-Fe based binary systems at the following initial conditions: 300K≤ T_o ≤ 900K, ΔT = 1÷10 K.

So, for a number of the elements forming the surface segregations in α-Fe under isothermal exposing in vacuum (due to internal adsorption), the experimental values of SFT from Table 5 and the simulated SST ones (T_{seg}) resultant from (10) are presented as functions on ΔG_{seg} in Fig. 12, where the solid lines are simulated, and the points being the experimental ones.

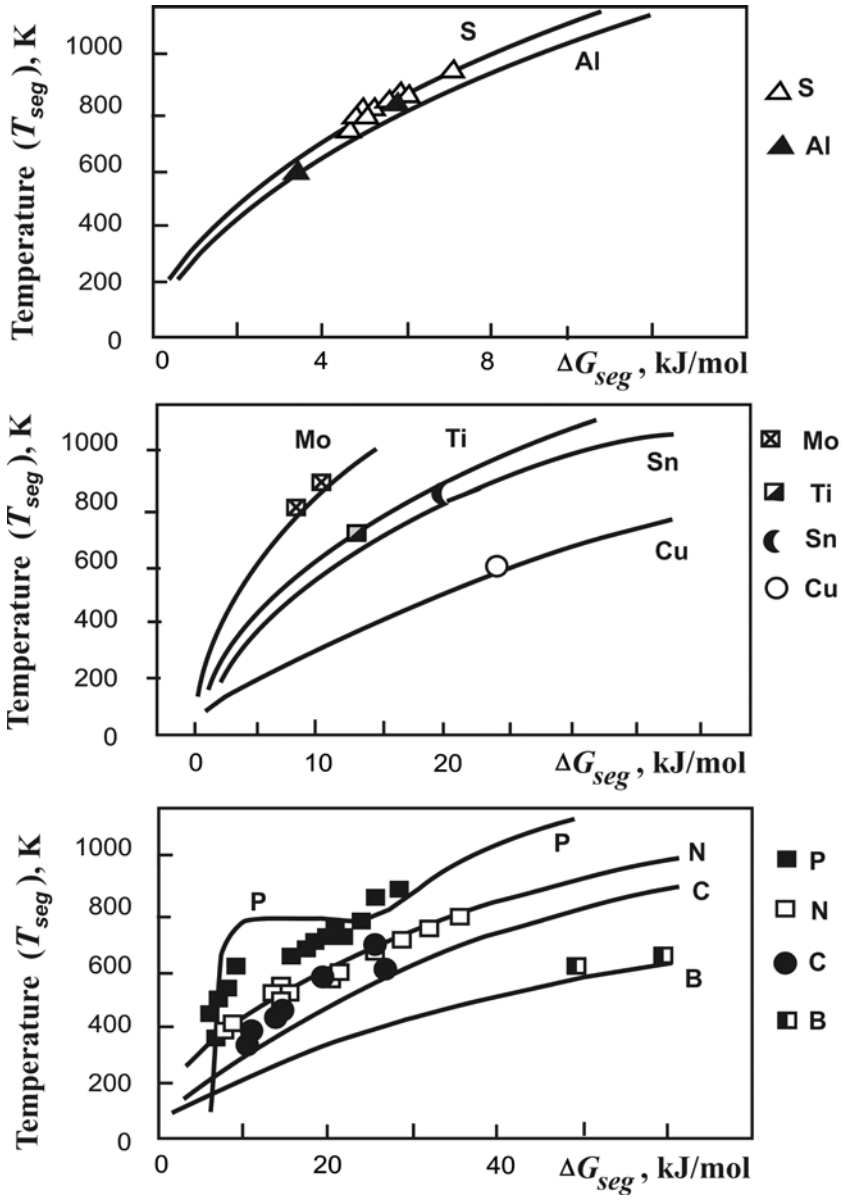

Fig. 12. Experimental (points) and computed (curves) data of the values of T_{seg} against ΔG_{seg} for a number of the elements segregating in the free surface of the investigated α-Fe alloys under isothermal exposing in vacuum.

There is correlation between the experimental points and the simulated curves shown in Fig. 12. Particularly, in the both cases the segregations of C, N, and B are forming in lower temperatures than those of P, Mo, Ti, Al, S, Sn, Cu; segregations of S and Al appear at higher temperatures than P and Mo segregating in the same interval. Again, the last figure (Fig. 12) illustrates the experimentally observed SFT values to be in relation with the thermodynamics parameter ΔG_{seg}, the latter in turn being dependent on the alloy composition. For notice: a relatively low level of SFT for Cu (Fig. 11) is probably due to a low value of the corresponding ΔG_{seg}, according to (9).

6. Conclusions

The obtained experimental data from Auger-spectroscopy method confirm that surface segregations of a solved element (C, N, B, P, Mo, Ti, Al, S, Sn, Cu) in α-Fe alloys under isothermal exposing in vacuum due to internal adsorption are formed in a certain temperature interval that can differ from those ones of the other solved elements. Particularly, it is shown that segregations of the elements such as C, N, B having the low values of activation energy of diffusion in α-Fe are forming in lower temperatures of exposing than those of the slower elements (P, Mo, Ti, Al, S, Sn, Cu) having the higher diffusion activation energies.

There was proposed a theoretical relationship between the temperature interval of forming the surface segregation of an element solved in α-Fe, the thermodynamics stimulus of its segregation (ΔG_{seg}), and its volume solubility change in respect of the temperature ($\partial X_{vo}(T)/\partial T$).

The obtained results can be important for metallurgical technologies using heat treatment to prevent intergranular failure of low carbon structural steels and maraging steels.

Acknowledgements. *This work financially supported by Russian Foundation for Basic Researches (Projects #16-08-00599 and #17-08-01193) and by State Task #2017/113 of Ministry of Education and Science of Russian Federation.*

References

[1] D. McLean, *Grain Boundaries in Metals* (Oxford University Press, London, 1957).
[2] E.D. Hondros, M.P. Seah // *Met. Trans.* **8A** (1977) 1363.
[3] P. Lejcek, *Grain Boundary Segregation in Metals* (Springer, Heidelberg, Germany, 2010).
[4] M.P. Seah, In: *Practical Surface Analysis by Auger and X-ray Photoelectron Spectroscopy*, ed. by D. Briggs and M.P. Seah (John Wiley & Sons, Chichester, 1983), Chapter 13.
[5] M. Guttmann, Ph. Dumoulin, M. Wayman // *Metallurgical Transactions* **13A(10)** (1982) 1693.
[6] M.P. Seah, C. Lea // *Scripta Metallurgica* **18(10)** (1984) 1057.
[7] A.I. Kovalev, V.P. Mishina, G.V. Scherbedinsky // *FMM* **62(1)** (1986) 126. (in Russian)
[8] A.I. Kovalev, V.P. Mishina // *Metallophysica* **9(4)** (1987) 45. (in Russian)
[9] Yu.G. Abashkin, A.P. Dementyev, T.M.Jibuty, O.P. Ivanova // *Poverhnost'. Rentgenovskie, Sinkhrotronnye I Neitronnye Issledovaniya (The Journal of Surface Investigation. X-ray, Synchrotron and Neutron Technique)* **11** (1989) 48. (in Russian)
[10] A.I. Kovalev, V.P. Mishina, G.V. Scherbedinsky // *Metallophysica* **9(3)** (1987) 112. (in Russian)
[11] K. Masuda-Tindo // *Phys. Stat. Sol. (B)* **134** (1986) 545.
[12] Ph. Dumoulin, M. Guttmann // *Materials Science and Engineering* **42(11-13)** (1979) 249.
[13] H.J. Grabke // *Materials Technology Steel Research* **57(4)** (1986) 178.

[14] B.L. Eyre, B.C. Edwards, J.M. Titchmarsh, In: *Adv. Phys. Met. and Appll. Steels Int. Conf.* (Chameleon press, London, 1982), p.246.
[15] O.A. Bannykh, P.B. Budberg, S.P. Alisova et al., *Phase Diagrams of Binary and Multicomponent Systems based on Ferrous* (Metallurgy, Moscow, 1966). (in Russian)
[16] O. Kubaschewski, *Iron-Binary Phase Diagrams* (Springer Verlag, Berlin, Heidelberg, Germany, 1982)
[17] C.B. Zemsky, D.A. Litvinenko // *FMM* **32(3)** (1971) 591. (in Russian)
[18] J. Wroblewski, J. Rasek, J.W. Morom // *Acta Phys. Pol. A* **A46(6)** (1974) 737. (Poland)
[19] S.A. Golovin, M.A. Krishtall, A.N. Svobodin // *Fizica i himia obrabotky materialov* (*Physics and Chemistry of Materials*) **1** (1968) 119. (in Russian)
[20] T. Matsuyama, H. Hosokawa, H. Suto // *Transactions of Japan Institute of Metals* **24(8)** (1983) 589.
[21] M.A. Krishtall, A.R. Mokrov // *Zash'ita Metalov* (*Protection of Metals*) **1** (1967) 18. (in Russian)
[22] A.M. Huntz, M. Aucouturier, P. Lacombe // *C.R. Acad. Sci*. **265(10)** (1967) 554.
[23] A. Vignes, J. Philibert, M. Badia, J. Levasseur, In: *Trans. 2nd Natl. Conf.: Electron Microprobe Analysis* (Boston University Press, Boston, 1967), Paper N20.
[24] P.L. Gruzin, V.V. Mural', A.P. Fokin // *FMM* **32(1)** (1971) 208. (in Russian)
[25] Y. Adda, J. Philibert, *La Diffusion Dans les Solides* (Par Saclay, Paris, 1966).
[26] V.A. Lazarev, V.M. Golikov // *FMM* **29(3)** (1970) 598. (in Russian).
[27] V.P. Shapovalov, A.N. Kurasov // *Metallovedenie i termicheskaya obrabotka metallov* (*Metal Science and Heat Treatment*) **9** (1975) 71. (in Russian)
[28] A.I. Kovalev, D.L. Wainstein, In: *Handbook of metallurgical Design*, ed. by G. Totten, Lin Xie and Kiyoshi Funatani (Marcel Dekker Inc., N.Y., U.S.A., 2004), p.57.